Rydberg atom driven by a sequence of two laser pulses: Ramsey interferometry

A. Wójcik and R. Parzyński
Quantum Electronics Laboratory, Institute of Physics, A. Mickiewicz University, Grunwaldzka 6, 60-780 Poznań, Poland
(Received 22 June 1994; revised manuscript received 1 December 1994)

Following the experiment of Jones *et al.* [Phys. Rev. Lett. **71**, 2575 (1993)], we present a theory of coherent redistribution of population in a model Rydberg atom exposed to a sequence of two identical laser pulses separated in time and shorter in duration than the Rydberg-electron Kepler period. For different initial-population conditions, we solve the problem of redistribution in a fully analytical and rigorously nonperturbative way, thus obtaining discrete-state population amplitudes, dependent on laser intensity, and a time delay between the pulses. Using this solution, we study the population in a given state versus pulse delay (Ramsey fringes), as well as the corresponding Fourier spectrum, for both low and high laser intensities. From the number of frequency components and their positions in the Fourier spectrum, we deduce the redistribution of the initial-state population over a number of states by the first pulse. Within our model calculations we achieve qualitative agreement with the experimental observation of Jones *et al.* that an increase in laser intensity results in a general increase in the number of frequency components in the Fourier spectrum. Our theoretical results are also consistent with the experimental finding of Noordam *et al.* [Phys. Rev. Lett. **68**, 1496 (1992)] that Raman transitions via the continuum between different Rydberg states are essential for population redistribution. We suggest new experiments to measure the effect of the initial-state depletion on the Fourier spectrum. As follows from our model calculations, some frequency components (both low and optical) present in the low-intensity Fourier spectrum should vanish in the high-intensity spectrum due to complete depletion of the initial state by the first pulse.

PACS number(s): 32.80.Rm, 42.50.Hz

I. INTRODUCTION

The Ramsey-like method, based on the effect of a sequence of two identical laser pulses separated in time by T on a given sample [1], has hitherto been used with success in, e.g., molecular spectroscopy [2]. Recently, Jones *et al.* [3] have demonstrated experimentally that this two-pulse method is also a good tool for monitoring coherent transfer of population from a well-isolated atomic state to a family of Rydberg states, as well as from a given Rydberg state to the nearest Rydberg neighbors. Briefly, in the Rydberg atom of our interest, the first laser pulse from the sequence, of duration shorter than the Kepler period, spreads at least a part of the population from the initial state over a large number of states, creating in this way a Rydberg wave packet. During the delay time T between the first and the second pulses, shorter than the natural decay time, all populated atomic states undergo free evolution and, due to different state energies $\hbar\omega_n$, they acquire different phases $\omega_n T$. Thus, when the second pulse comes, it encounters the population redistributed by the first pulse over states whose phases depend on the delay time T. Due to the existing redistribution, the second pulse can transfer the population to a selected state along a number of paths, each path originating in a different state of nonzero population after the first pulse. As a result, the population in a given state after the two-pulse sequence is the effect of interference sensitive to the phases of the states involved. It leads to variations of population in a given state as a function of the delay T between the pulses. These temporal variations of population are analogs of the light intensity variations at the output of an ordinary optical Mach-Zender interferometer. The temporal variations include all frequencies corresponding to energy differences between any two atomic states having a nonzero population after the first pulse. All these frequency components, inherent in the variation of a given state population, can be identified by Fourier analysis. On the basis of the frequency components found, we can identify all states of a nonzero population after the first pulse. Thus the two-pulse method can serve as a tool for studying the redistribution of the initial population by the first laser pulse. It is an advantage of this method that it allows us to deduce the redistribution over a number of states by measuring the population in one state only. As shown in the experiment by Jones *et al.* [3], this method is extremely useful, particularly when combined with the field-ionization method of detection of the Rydberg-state population [4].

In the paper of Jones *et al.* [3] two experiments with potassium atoms were reported, differing from each other in the choice of the initial atomic state. In both experiments two identical 772-nm laser pulses were used, each of 100 fs duration, and intensity of the order of 10^{11} W/cm^2 and higher, delayed by up to 40 ps. In the first experiment the initial state was the $3d$ state from which a coherent superposition of nf Rydberg states ($12 < n < 22$) was excited by the first pulse. After the second pulse, the population in the $16f$ Rydberg state was measured versus the delay time T, and in the corresponding Fourier transform a general increase in the number of frequency components with increasing laser intensity was observed.

This was experimental evidence for a growing number of Rydberg states populated by the first pulse with its increasing intensity. In the second experiment the initial state was a single Rydberg nl eigenstate ($n>12$, $l=0-3$), each of the nf states ($12<n<18$) being resonant with the lower $3d$ state within the bandwidth of the laser pulse used. In particular, the population in the $18f$ state, after the interaction of the initial $15f$ Rydberg state with two laser pulses, was measured as a function of the delay T. A number of frequency components in the Fourier transform of the $18f$ population were observed, which testified to the redistribution of the initial $15f$ population over several neighboring Rydberg states by the first pulse. In this experiment, the redistribution was seen to proceed via the two-photon Raman channel employing the lower resonant $3d$ state as an intermediary. It is worth noting that this kind of Rydberg-state redistribution via a lower bound state stands in contrast to the redistribution via the atomic continuum, previously observed in barium atoms by Noordam *et al.* [5]. Quite recently we have shown [6] that the redistribution via a lower resonant state significantly affects the phenomenon called the interference stabilization of the Rydberg atom against intense laser ionization [7–16].

In their experiments Jones *et al.* used relatively intense pulses significantly depleting the initial atomic state; consequently, their observations could not be interpreted in terms of the perturbation theory of Noordam, Duncan, and Gallagher [4]. The authors however, were able to reproduce the temporal variations observed and the corresponding Fourier spectra using numerical integration of the Schrödinger equation for Gaussian pulses, within a finite basis of 22 discrete states ($3d, 14p, \ldots, 20p$, $11f, \ldots, 24f$), ignoring photoionization from both the $3d$ and Rydberg states. In contrast to the above numerical treatment, in this paper we present a purely analytical and nonperturbative approach to the problem of interaction between a sequence of two delayed laser pulses and the Rydberg atom. The model of interaction we consider takes into account both ionization loss of Rydberg states and two-photon Raman couplings via the continuum between any two Rydberg states. Within this model we study the effect of laser intensity on the redistribution of the initial population, localized in a single state only, over a number of states. We succeed in obtaining—within the analytical model—close qualitative agreement with the experimental findings of Jones *et al.* The main result of our solution is the reproduction of the tendency of the number of frequency components in the Fourier spectrum of a given-state population variation to increase with increasing laser intensity, as observed by Jones *et al.* However, in contrast to this general tendency, we found that some frequency components, present in the low-intensity Fourier spectrum, actually vanish in the high-intensity spectrum due to a complete removal of the population from the initial state by the first pulse. We present this theoretical prediction as our suggestion for future experiments. We also give results, obtained within our model, that are consistent with the experiment of Noordam *et al.* [5] on Rydberg-state redistribution via atomic continuum.

II. MODEL AND ANALYTICAL SOLUTION

Our atomic model is shown in Fig. 1. It includes a quasicontinuum $\{|j\rangle\}$ of Rydberg states of the same parity, a lower-lying state $|e\rangle$ of opposite parity, which is nearly resonantly coupled to the quasicontinuum, and an upper-lying flat continuum $|c\rangle$. Besides j and e we introduce the index n, covering all discrete states of the model, i.e., those for which $\{n\}=\{e,\{j\}\}$. We aim at obtaining a general solution for this model, which then could be specified for the two particular cases studied by Jones *et al.* Therefore, at the very beginning, we do not determine which discrete state ($|e\rangle$ or $|j_0\rangle$) is initially, at $t=0$, populated. Applying a rectangular pulse and rotating-wave approximations, we start with the Laplace-transformed Schrödinger equation for discrete states of our model [6]:

$$\left[s+i\frac{E_n}{\hbar}\right]\tilde{b}_n=-i\sum_{n'}\Omega_{nn'}\tilde{b}_{n'}-\sum_{j'}\delta_{nj}\bar{\Gamma}_{jj'}\tilde{b}_{j'}+b_n(0)\ . \quad (1)$$

Here s denotes the Laplace variable, $\tilde{b}$ the Laplace transform of the Schrödinger population amplitude, $b(0)$ the initial value of the amplitude at $t=0$, δ_{nj} the Kronecker delta function, $\Omega_{nn'}=\langle n|V|n'\rangle/\hbar$ the Rabi frequency for the transition between a quasicontinuum state and the state below it, and $\bar{\Gamma}_{jj'}=(1+iq_{jj'})\Gamma_{jj'}/2$ the two-photon Raman coupling between any two Rydberg states via the continuum with $\Gamma_{jj'}=(2\pi/\hbar)V_{jc}V_{cj'}\rho$, with ρ the continuum state density, V the atom-photon interaction Hamiltonian, and $q_{jj'}$ the Fano parameter. In the search for a compact solution of Eq. (1), the dependence of the Fano parameter on the quasicontinuum indices j and j' proves to be an obstacle. However, bearing in mind that matrix elements involving different Rydberg states of the same angular momentum are scaled by the principal quantum number in the power of $-\frac{3}{2}$, we factorize these elements as $V_{\alpha j}=f_j V_\alpha$ with V_α being a constant for a wide group of Rydberg states. With this factorization ansatz, the Fano parameter is rendered independent of the Rydberg quasicontinuum index ($q_{jj'}=q$) and, moreover, $\Omega_{ej}=f_j\Omega_e=f_j\Omega$ and $\bar{\Gamma}_{jj'}=f_j f_{j'}\bar{\Gamma}$, where

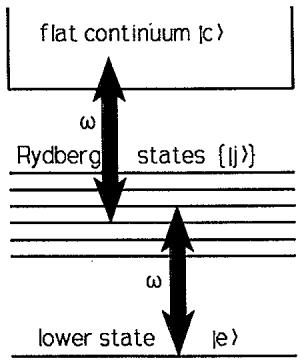

FIG. 1. The atomic model under study with Rydberg states $\{|j\rangle\}$, a lower-lying state $|e\rangle$, and a flat continuum $|c\rangle$. The initially populated state is either the $|e\rangle$ state or a given $|j_0\rangle$ Rydberg state.

$\bar{\Gamma}=(1+iq)\Gamma/2$ with Γ having the sense of an ionization rate. Then, after the energy origin is shifted so that $E_e=0$, Eq. (1) splits into the set

$$s\tilde{b}_e=-i\Omega\sum_j f_j\tilde{b}_j+b_e(0)\ , \tag{2}$$

$$(s-i\delta_j)\tilde{b}_j=-i\Omega\tilde{b}_e f_j-\bar{\Gamma}f_j\sum_{j'}f_{j'}\tilde{b}_{j'}+b_j(0)\ , \tag{3}$$

where δ_j is the detuning of the laser frequency from the frequency of the atomic transition between the $|j\rangle$ level in the quasicontinuum and the $|e\rangle$ level below it. To solve the set obtained, we first combine Eq. (2) with Eq. (3), then divide the resulting equation by $s-i\delta_j$ and multiply it by f_j, and finally sum over all j. In this way we find that

$$\sum_j f_j\tilde{b}_j=\frac{-i\Omega S b_e(0)+s\sum_{j'}\dfrac{f_{j'}b_{j'}(0)}{s-i\delta_{j'}}}{s(1+\bar{\Gamma}S)+\Omega^2 S}\ , \tag{4}$$

where

$$S=\sum_{j'}\frac{f_{j'}^2}{s-i\delta_{j'}}\ . \tag{5}$$

Using Eq. (4), we calculate $\tilde{b}_e$ from Eq. (2) and then $\tilde{b}_j$ from Eq. (3), arriving at

$$\tilde{b}_e=\frac{b_e(0)+A}{s(1+\bar{\Gamma}S)+\Omega^2 S}\ , \tag{6}$$

$$\tilde{b}_j=\frac{b_j(0)}{s-i\delta_j}-\frac{f_j}{s-i\delta_j}\frac{i\Omega b_e(0)+\bar{\Gamma}\sum_{j'}f_{j'}b_{j'}(0)+B}{s(1+\bar{\Gamma}S)+\Omega^2 S}\ , \tag{7}$$

where

$$A=\sum_{j'}\frac{[\bar{\Gamma}f_{j'}b_e(0)-i\Omega b_{j'}(0)]f_{j'}}{s-i\delta_{j'}}\ , \tag{8}$$

$$B=\sum_{j'}\frac{(\Omega^2+i\bar{\Gamma}\delta_{j'})f_{j'}b_{j'}(0)}{s-i\delta_{j'}}\ . \tag{9}$$

To transform the above s-dependent solutions for $\tilde{b}_e$ and $\tilde{b}_j$ to the time domain, we perform a specific modeling of the Rydberg quasicontinuum. Assuming that we are interested in a highly excited Rydberg quasicontinuum, we roughly approximate it by the Bixon-Joertner structure (see, e.g., [6] and [17]), i.e., by a set ($j=0,\pm1,\pm2,\ldots$) of equidistant levels with spacing $\hbar\Delta$, coupled to the lower $|e\rangle$ state and to the continuum with strengths independent of the quasicontinuum index ($f_j=1$). Then, $\delta_{j'}=\delta_0-j'\Delta$ and S defined by Eq. (5) can be summed analytically with the result

$$S=\frac{\pi}{\Delta}\frac{1+\mu}{1-\mu}\ , \tag{10}$$

where $\mu=\exp[t_r(i\delta_0-s)]$ with $t_r=2\pi/\Delta$ being the classical round-trip time of the Rydberg electron. With S in the form of Eq. (10), our solution for the Laplace transforms $\tilde{b}_e$ and $\tilde{b}_j$ can be transformed to the time domain fully analytically, applying the power-series method of Stey and Gibberd [6,17]. In our case, this method, for the expression $1/[s(1+\bar{\Gamma}S)+\Omega^2 S]$, inherent in Eqs. (6) and (7), must be expanded in a Taylor series with respect to μ. Each term in this expansion is then found to have a simple time representation, while the maximum number of terms that have to be included is limited by the actual interaction time between the atom and photons. In the experiment of Jones *et al.* [3], the laser pulses of $t_p=100$ fs duration were shorter than the round-trip time t_r of the electron in the populated Rydberg states. For such a short pulse ($t_p/t_r=\tau\le1$), to be of our exclusive interest throughout the rest of this paper, only the first term in the above-mentioned expansion needs to be included. Formally, it leads to the replacement

$$\frac{1}{s(1+\bar{\Gamma}S)+\Omega^2 S}\xrightarrow{\tau\le1}\frac{1}{1+\pi v}\frac{1}{s+\rho\Delta}\ , \tag{11}$$

where $\rho=\pi u/(1+\pi v)$, $u=(\Omega/\Delta)^2$, and $v=\bar{\Gamma}/\Delta$. The parameters u and v are dimensionless and depend on laser intensity in a linear way. The first parameter describes the strength of coupling of the lower $|e\rangle$ state to the Rydberg quasicontinuum, whereas the parameter v gives the strength of coupling of the Rydberg quasicontinuum to genuine continuum. Following Eq. (11), we replace our general equations (6) and (7) by their short-pulse counterparts

$$\tilde{b}_e=\frac{b_e(0)}{1+\pi v}\frac{1}{s+\rho\Delta}+\frac{\Delta}{1+\pi v}\sum_j[vb_e(0)-i\sqrt{u}\,b_j(0)]\tilde{g}_j\ , \tag{12}$$

$$\tilde{b}_j=\frac{b_j(0)}{s-iy_j\Delta}-\frac{\Delta}{1+\pi v}\left[i\sqrt{u}\,b_e(0)+v\sum_{j'}b_{j'}(0)\right]\tilde{g}_j+i\frac{\Delta}{1+\pi v}\sum_{j'}\frac{w_{j'}b_{j'}(0)}{y_{j'}-y_j}(\tilde{g}_{j'}-\tilde{g}_j)\ , \tag{13}$$

where $y_j=\delta_j/\Delta=y_0-j$, $y_0=\delta_0/\Delta$, $w_j=u+ivy_j$, and

$$\tilde{g}_j=\frac{1}{(s+\rho\Delta)(s-iy_j\Delta)}\ . \tag{14}$$

Transforming straightforwardly the above $\tilde{g}_j$ to the time domain, we finally arrive at the Schrödinger population amplitudes $b(t_p)$ at the end of the short pulse ($\tau=t_p/t_r\le1$). These after-pulse amplitudes $b(t_p)$ turn out to be related to the initial before-pulse amplitudes $b(0)$ as

$$b_e(t_p)=\sum_n R_{en}(t_p)b_n(0)=R_{ee}(t_p)b_e(0)+\sum_j R_{ej}(t_p)b_j(0)\ , \tag{15}$$

$$b_j(t_p)=\sum_n R_{jn}(t_p)b_n(0)=R_{je}(t_p)b_e(0)+\sum_{j'}R_{jj'}(t_p)b_{j'}(0)\ , \tag{16}$$

where $R_{nn'}(t_p)$ are the elements of the evolution matrix

$$R_{ee}(t_p)=\frac{e^{-2\pi\rho\tau}}{1+\pi v}-2\pi v\sum_j K_j(\tau)\ , \tag{17}$$

$$R_{ej}(t_p)=R_{je}(t_p)=i2\pi\sqrt{u}\,K_j(\tau)\ , \tag{18}$$

$$R_{jj'}(t_p)=\delta_{jj'}\left[e^{i2\pi y_j\tau}-\frac{(2\pi)^2}{(1+\pi v)z_j}[uK_j(\tau)+w_j\tau e^{i2\pi y_j\tau}]\right]+2\pi(1-\delta_{jj'})\left[vK_j(\tau)-iw_{j'}\frac{K_{j'}(\tau)-K_j(\tau)}{y_{j'}-y_j}\right]\ , \tag{19}$$

with

$$K_j(\tau)=\frac{e^{i2\pi y_j\tau}}{1+\pi v}\frac{e^{-z_j\tau}-1}{z_j} \tag{20}$$

and $z_j=2\pi(\rho+iy_j)$.

The above fully analytical short-pulse ($\tau\leq 1$) amplitudes will be now applied to a sequence of two identical laser pulses separated in time by T. This is exactly the same as in the experiments of Jones *et al.* [3]. Starting from the initial population amplitudes $\{b_n,(0)\}$ we get, according to Eqs. (15) and (16), the following population amplitudes $\{b_n(t_p)\}$ after the first pulse:

$$b_n(t_p)=\sum_{n'} R_{nn'}(t_p)b_{n'}(0)\ , \tag{21}$$

where n' runs over all discrete states of the model. Then, in a time T (much shorter than the spontaneous decay times) between the pulses, the atom is left free. Due to free evolution, the amplitudes at the time t_p+T, when the second pulse comes, become

$$b_n(t_p+T)=e^{-i(\omega_n-i\gamma_n/2)T}b_n(t_p)\ , \tag{22}$$

where ω_n are atomic eigenfrequencies and γ_n spontaneous decay rates. The amplitudes (22) form the new initial conditions that are encountered by the second pulse. Because the second pulse is of the same duration as the first pulse, the amplitudes after the two-pulse sequence are

$$b_n(2t_p+T)=\sum_{n'} R_{nn'}(t_p)b_{n'}(t_p+T)\ . \tag{23}$$

Combining Eqs. (21)–(23), we finally express the last amplitudes as

$$b_n(2t_p+T)=\sum_{n'} D_{nn'}(t_p)e^{-i(\omega_{n'}-i\gamma_{n'}/2)T}\ , \tag{24}$$

where

$$D_{nn'}(t_p)=R_{nn'}(t_p)\sum_{n''}R_{n'n''}(t_p)b_{n''}(0)\ . \tag{25}$$

Multiplying Eq. (24) by its complex conjugate, we find the population in a given discrete state after the two-pulse sequence $P_n(T)$ versus the delay time T to be

$$P_n(T)=\sum_{n',m'} D_{nn'}(t_p)D^*_{nm'}(t_p)e^{-i\omega_{n'm'}T}e^{-\gamma_{n'm'}T}\ , \tag{26}$$

where $\omega_{n'm'}=\omega_{n'}-\omega_{m'}$ is the differential frequency between any two atomic eigenfrequencies, whereas $\gamma_{n'm'}=(\gamma_{n'}+\gamma_{m'})/2$. As seen from Eq. (26), there are three kinds of oscillating terms in a given-state population variation $P_n(T)$: (i) a zero-frequency term if $n'=m'$, (ii) a low-frequency term if n' and m' label two different Rydberg states, and (iii) a high-frequency (optical) term if one of the two indices corresponds to a given Rydberg state and the other one to the $|e\rangle$ state below Rydberg quasicontinuum. By taking the Fourier transform of Eq. (26) we are able to extract all these differential frequencies present in a given-state population variation

$$P_n(\omega)=\frac{1}{\sqrt{2\pi}}\int_0^T P_n(T)e^{-i\omega T}dT=\frac{1}{\sqrt{2\pi}}\sum_{n',m'} D_{nn'}(t_p)D^*_{nm'}(t_p)\times\frac{\gamma_{n'm'}-i(\omega+\omega_{n'm'})}{(\omega+\omega_{n'm'})^2+(\gamma_{n'm'})^2}\ . \tag{27}$$

In the Fourier spectrum $|P_n(\omega)|$, each differential frequency will be distinguished by a peak. From the number of peaks and their positions in the Fourier spectrum of a given n-state population variation one can conclude about *all* states over which the initial population has been distributed by the first pulse and those contributing to the n-state population during the action of the second pulse. Equations (26) and (27) are the key equations of our paper. They have two main advantages. First, as obtained in a fully nonperturbative way, they are valid for arbitrary intense laser pulses not violating the assumed rotating-wave approximation. As a matter of fact, intensity effects in the redistribution of the initial population is what we shall study in the next section. Second, they apply to any initial-population conditions. Obviously, Eqs. (26) and (27) become substantially simplified when these initial conditions are specified. Following the experiments of Jones *et al.*, the initial population will be further assumed to be in a single state only, either the lower state $|e\rangle$ or a given Rydberg state $|j_0\rangle$. This corresponds to setting in Eq. (25) $b_{n''}(0)=\delta_{n''e}$ or $b_{n''}(0)=\delta_{n''j_0}$. In both cases the summation over n'' in Eq. (25) is reduced to only a single term, resulting in a relatively simple form of $D_{nn'}(t_p)$.

III. RESULTS AND INTERPRETATION

Now we apply our key equations (26) and (27), along with Eqs. (25) and (17)–(20), to f Rydberg states in potassium. The situation corresponds to the case experimentally studied by Jones *et al.* However, to fulfill approximately the condition of uniform level spacing, under which our evolution matrix $R_{nn'}(t_p)$ was calculated, we deal with higher Rydberg levels than in the abovementioned experiment, namely, with those around the $40f$ level. We take the required spontaneous decay rates of these Rydberg levels, as well as of the $3d$ level, from [18]. The level next to $40f$ is separated from the latter by $\Delta=(E_{41f}-E_{40f})/\hbar=6.2\times10^{11}\ \mathrm{s}^{-1}$, corresponding to $3.31\ \mathrm{cm}^{-1}$, and we take this Δ as a unit to scale the spacing between any pair of levels. The above Δ gives the classical Kepler round-trip time of the Rydberg electron

equal to $t_r \simeq 10$ ps, which we choose as a unit of time to scale laser pulse duration t_p and the delay T between the pulses. Unless stated otherwise, the results presented correspond to the pulse duration 5 times shorter than the Kepler period, that is, $\tau = t_p/t_r = 0.2$. In all cases the Fano parameter $q = 0$ is assumed.

Our main results are represented in the form of two kinds of plots. One presents the variation of population in a given state as a function of delay between the two laser pulses, calculated with the use of Eq. (26), and the other is the Fourier spectrum of these variations, calculated from Eq. (27). As explained in Sec. II, both kinds of plots provide us with the information about the redistribution of the initial population over a number of states after the first pulse. It is striking that we can deduce this redistribution by analyzing the population after two pulses in a single state only, not in all. Because these plots are made for different laser intensities, they inform us about the effect of intensity on this distribution. There are three main aims of this presentation: first, to show that by neglecting photoionization losses our model gives results that qualitatively reproduce the tendencies observed in the experiment of Jones *et al.* [3] for potassium; second, to show that the inclusion of atomic continuum and Raman transitions via this continuum leads to results consistent with the experimental observations of Noordam *et al.* [5] for barium; third, to stimulate future experiments by making theoretical predictions, particularly in the region of laser intensities ensuring considerable depletion of the initial state, i.e., in the region accessible for studying only by the use of rigorous nonperturbative methods. All our results and the physics residing in our plots are qualitatively interpreted in terms of the interference of different Feynman transition paths.

A. 3*d* Initial-state case with no ionization

Figures 2 and 3 correspond to one of the two situations of the experiment of Jones *et al.* [3], namely, when initially the entire population was in the $|e\rangle = |3d\rangle$ state below the f Rydberg series and the ionization of Rydberg states was negligible, meaning $v = 0$. We assume the laser frequency to be resonant with the $3d \rightarrow 40f$ transition. However, for pictorial purpose we diminish the actual $3d$-$40f$ transition frequency (4062Δ) by a factor of 200. Under these conditions we demonstrate in Fig. 2 the calculated population in the $42f$ Rydberg state $P_{42f}(T)$ as a function of the scaled delay T/t_r between the two laser pulses, for three different laser intensities fixed by the parameter $u = (\Omega_{40f,3d}/\Delta)^2$. Figure 2(a) corresponds to what we call the low-intensity case ($u = 0.01$), Fig. 2(b) to the moderate-intensity case ($u = 0.5$), and Fig. 2(c) to the high-intensity case ($u = 1$). In the low-intensity case, the $42f$ population evolution is seen to be almost completely governed by rapid oscillations with optical frequency $\omega_{40f,3d}/200 + \omega_{42f,40f} = 22.24\Delta$. The amplitude of these rapid oscillations is only very weakly modulated by low differential frequencies between Rydberg states. In the moderate-intensity case, we observe well-pronounced low-frequency Rydberg oscillations in addition to optical oscillations. In the high-intensity case, a practically complete disappearance of optical oscillations is observed and only low-frequency Rydberg oscillations remain. The reason for the gradual vanishing of fast optical oscillations with increasing intensity is made clear when one recalls that the only oscillations present in a given state population are those with frequencies corresponding to the energy difference between states of nonzero population after the first pulse. In Fig. 2(d) we show the population left in the initial $3d$ state after the first pulse versus

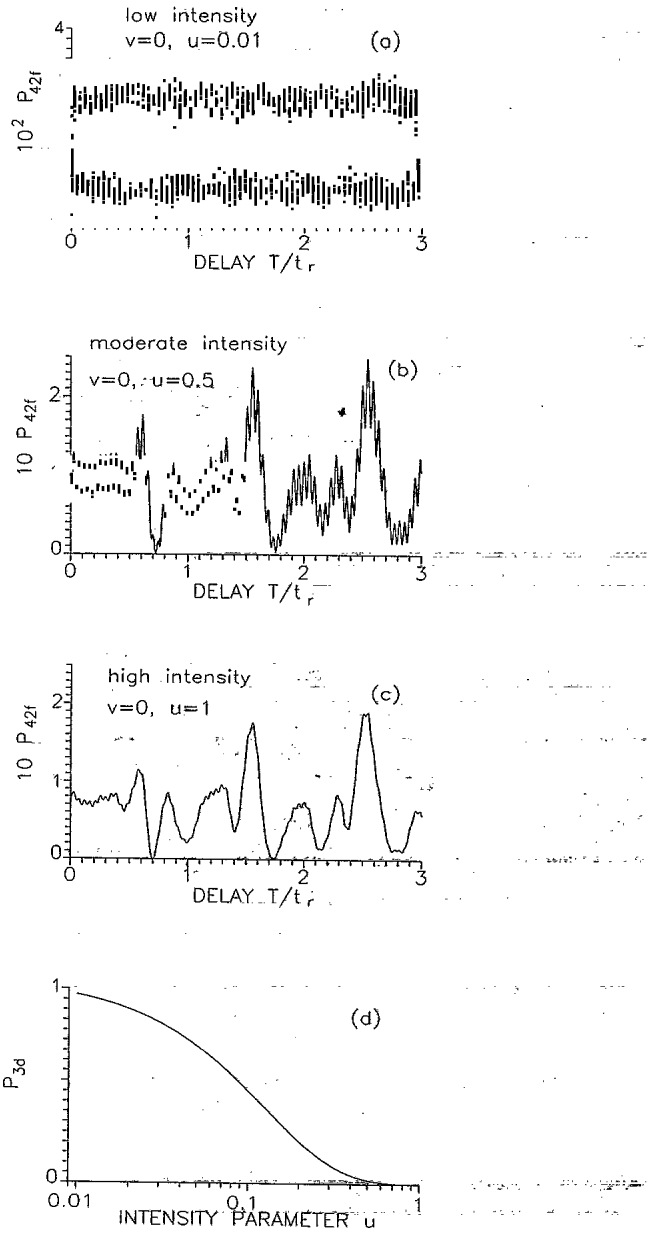

FIG. 2. The $42f$ Rydberg-state population in potassium as a function of the delay between two identical laser pluses of duration $\tau = 0.2$, for different laser intensities fixed by u. The initial state for the excitation is $3d$, the laser frequency is resonant with the $3d \rightarrow 40f$ transition, and there is no Rydberg-state ionization ($v = 0$). To resolve rapid optical oscillations, the actual $3d$-$40f$ transition frequency was diminished by a factor of 200. In (d), we show the $3d$ state population after the first pulse versus the pulse intensity.

laser intensity, calculated with the use of Eqs. (15) and (17). We see from Fig. 2(d) that in the high-intensity case ($u=1$), the initially populated $3d$ state has become almost completely depleted by the first pulse. It removes optical oscillations from the $42f$ state population. The general conclusion resulting from Fig. 2 is thus that, with increasing laser intensity, the initially dominant rapid optical oscillations become damped and finally replaced by slow Rydberg oscillations due to the transfer of the entire population from the $3d$ state to Rydberg states by the first pulse. We calculated the population variations in the other nf Rydberg states ($35 \leq n \leq 45$) as well and we always observed the same effect. In Sec. III B we will point to a similar depletion effect, but in the case when the initially populated is a given Rydberg state rather than the lower-lying $3d$ state.

Figure 3 shows the appropriate Fourier transform $|P_{42f}(\omega)|$ of the $42f$ state population variations from Fig. 2, for the two limiting cases, namely, the low-intensity ($u=0.01$) and the high-intensity ($u=1$) cases. The frequency scale in this figure covers all eigenfrequency differences between any two f Rydberg states from the $35f$-$45f$ interval. In the low-intensity case [Fig. 3(a)], only seven main frequency components are observed in the spectrum, all corresponding to the eigenfrequency differences between $42f$ and other Rydberg states. The components related to the $42f$-$40f$ and $42f$-$41f$ eigenfrequency differences are dominant. We checked that $40f$ and $41f$ are the states, nearest to the $42f$ state, that are most effectively populated by the first pulse. We observed at higher intensities that these seven components became more intense and, moreover, new components

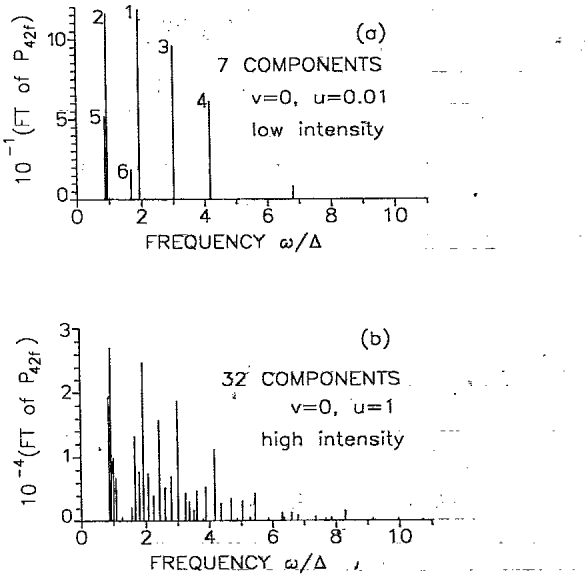

FIG. 3. Fourier transform (FT) of the $42f$ state population variations from Fig. 2. The number at a given peak corresponds to the energy difference between the Rydberg states: (1) $42f$-$40f$, (2) $42f$-$41f$, (3) $42f$-$39f$, (4) $42f$-$38f$, (5) $42f$-$43f$, (6) $42f$-$44f$, and (7) $42f$-$36f$.

built up. Some of these new components were found to correspond to the eigenfrequency differences between Rydberg states, none of which was the $42f$ state. In the high-intensity case [Fig. 3(b)], a dramatic increase in the number of frequency components is reported. Now, there are as many as 32 main frequency components including the component corresponding to the eigenfrequency difference between Rydberg states as distant as $43f$ and $35f$. We should stress that the general increase, presented in Fig. 3, in the number of frequency components in the Fourier spectrum with increasing laser intensity, obtained from our theory, is in qualitative agreement with the experimental observation of Jones *et al.* [3] for the lower $16f$ state. The increased number of frequency components proves that with increasing intensity, more and more Rydberg states, from the interval $35f$-$45f$, become partially populated due to the first pulse. We went on further with laser intensity ($u>1$) and still observed a formation of additional low-frequency peaks in the Fourier spectrum, including the peak corresponding to the $35f$-$45f$ eigenfrequency difference as well. This is the highest possible frequency for the state interval considered. However, what was more interesting was that all the peaks tended to become distinctly lower than the highest peak in Fig. 3(b). Such lowering of peaks means that at $u>1$, and particularly $u \gg 1$, part of the initial $3d$ population is sent by the first pulse also to Rydberg states different from those from the $35f$-$45f$ interval considered. This implies that at high intensities a number of Rydberg states participate in the redistribution of the initial population by the first pulse and that the description of this redistribution within atomic models with an overlimited number of states can by no means be correct.

The increasing complexity of the $42f$ state population variation (and of the corresponding Fourier spectrum as well) with an increase in laser intensity, as shown in Figs. 2 and 3, can be qualitatively understood in terms of the interference of different excitation paths. Generally speaking, all excitation paths can be divided into direct and indirect. Along the direct path, the $42f$ state is one-photon excited from the lower $3d$ state either by the first or the second pulse. In the indirect path, any nf Rydberg state different from the $42f$ state is one-photon excited by the first pulse and then the second pulse transfers the population from this state to the final $42f$ state in a two-photon Raman process. As a result, any indirect path engages as many as three photons, in contrast to a single photon engaged in any direct path. On this basis we can conclude that for an indirect path to be revealed, intensities higher than for a direct path are required. Thus, what we can expect at low intensities is just interference between two direct paths (direct-direct) leading to modulation of the $42f$ state population with optical frequency ($\omega=\omega_{42f}-\omega_{3d}$). At higher intensities, interference between any direct path and any indirect path (direct-indirect) comes into play, leading to the modulation with non-optical frequencies equal to the differences between eigenfrequencies of the $42f$ state and any other Rydberg state ($\omega=\omega_{42f}-\omega_{nf}$, $n\neq 42$). At high intensities, the interference between any two indirect paths

(indirect-indirect) becomes possible, leading here to modulation with frequencies corresponding to the difference between eigenfrequencies of any two Rydberg states, none of which is the final $42f$ state ($\omega=\omega_{nf}-\omega_{mf}$, $n\neq m\neq 42$). This is exactly the tendency that is consistent with what we see in Figs. 2 and 3. In terms of interference, we can also explain the vanishing of optical modulation at high intensities, shown in Fig. 2(c). As follows from Fig. 2(d), at high intensities the initial $3d$ state has become completely depleted by the first pulse and the direct $3d$-$42f$ path is closed for the second pulse. As a result, there is no direct-direct interference, leading to optical modulation.

B. $40f$ initial-state case with no ionization

Figures 4 and 5 correspond to another experimental situation of Jones *et al.* [3], namely, the one with the whole initial population in a given Rydberg state resonant with the lower $3d$ state. In our case, $40f$ is chosen to be the initially populated Rydberg state. Under this initial condition, as well as under the neglect of Rydberg state photoionization ($v=0$), we show in Fig. 4 the calculated $42f$ Rydberg-state population versus a delay between the laser pulses and in Fig. 5 the corresponding Fourier transform for two strikingly dissimilar laser intensities. At a low laser intensity ($u=0.01$), rapid optical oscillations are seen to be modulated by only one low frequency equal to the $42f$-$40f$ eigenfrequency difference. At a high intensity ($u=1$), the time variations of the $42f$ population become increasingly complicated, exhibiting an increase in the number of low-frequency components up to 24. This theoretically predicted tendency again agrees qualitatively with the experimental observation of Jones *et al.* for the $18f$ state population if the initially populated is the $15f$ Rydberg state. This is the proof that more and more Rydberg states close to the initial $40f$ state receive some population due to increasing intensity of the first pulse. In this case, the redistribution channel includes the lower $3d$ state as an intermediary.

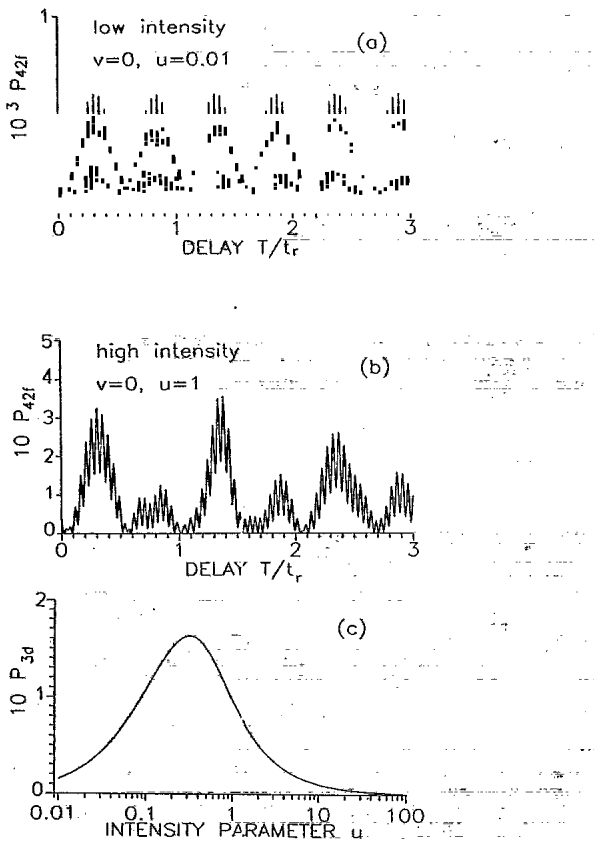

FIG. 4. The $42f$ Rydberg-state population as a function of the delay between two pulses under the assumption that initially the entire population is in the $40f$ state. This is a case of no photoionization of Rydberg states ($v=0$). All other conditions are the same as in Fig. 2. In (c) we show the $3d$ state population after the first pulse versus the pulse intensity.

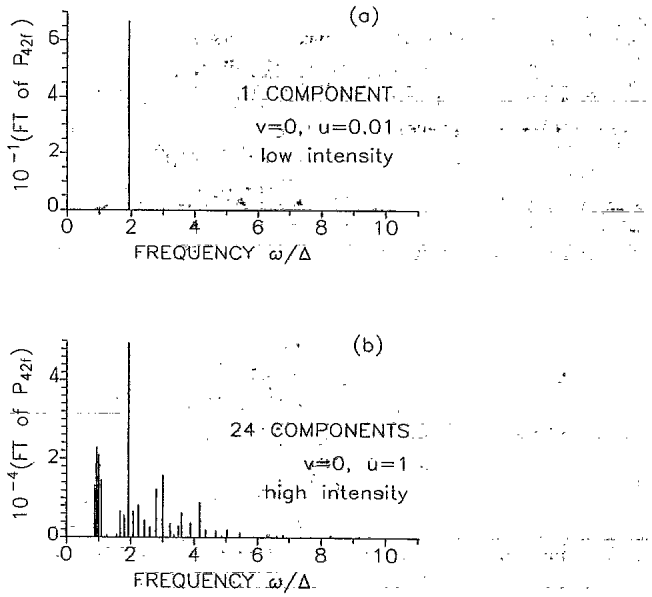

FIG. 5. Corresponding Fourier spectra of the time variations in Fig. 4.

Also in this case, as in Sec. III A, the interference point of view is very useful in understanding what we see in Figs. 4 and 5. Now, however, there are different elementary transition paths. In the direct path, the atom from the initial $40f$ Rydberg state is transferred to the final $42f$ Rydberg state due to a two-photon Raman process, caused by either the first or the second pulse. Contrary to the considerations presented in Sec. III A, there are now two kinds of indirect paths, the lower-order and the higher-order paths. In the lower-order indirect path, the atom is sent by the first pulse from the initial $40f$ state to the lower $3d$ state and then the second pulse sends it to the final $42f$ state. Thus the lower-order indirect path engages two photons, which is exactly the same number of photons as the direct path. In the first step of the higher-order indirect path, the atom from its initial $40f$ state is transferred by the first pulse to any nf Rydberg states ($n\neq 42$) in a two-photon Raman process. In the second step, the second pulse sends the atom from the previously populated nf state ($n\neq 42$) to the final $42f$ state, again in a two-photon Raman process. As a result, the higher-order indirect path engages four photons and to be effective it needs intensities higher than all other

two-photon paths. Thus, at low intensities we expect mutual interferences between the two direct paths—the one engaging photons from the first pulse and the other from the second pulse—and the lower-order indirect paths. The interference of the two direct paths leads to the modulation at the low differential frequency $\omega=\omega_{42f}-\omega_{40f}$. Any direct path interferring with the lower-order indirect path results in fast optical oscillations at $\omega=\omega_{42f}-\omega_{3d}\simeq\omega_{40f}-\omega_{3d}$. This explains why in Fig. 4(a) we observe optical oscillations with only one superimposed low-frequency modulation at $\omega=\omega_{42f}-\omega_{40f}$. At higher intensities, the higher-order indirect paths start to contribute. Any higher-order indirect path interferes with all two-photon paths at moderate intensities and with all other higher-order indirect paths at high intensities. Consequently, additional low-frequency components are generated in the spectrum, namely, $\omega=\omega_{42f}-\omega_{nf}$, $\omega_{40f}-\omega_{nf}$, and $\omega_{nf}-\omega_{mf}$ with $n\neq m\neq 40$ and 42. This is exactly what we can see in Fig. 5(b). Going back to Fig. 4(b) and comparing it with Fig. 4(a), we see the disappearance of optical oscillations. This suggests that at high intensities ($u>1$) the lower-order indirect path ($40f \xrightarrow[\text{1st pulse}]{} 3d \xrightarrow[\text{2nd pulse}]{} 42f$) stops contributing. In Fig. 4(c) we show that the reason for the closing of this path is a monotonic decrease of the $3d$ population after the first pulse at high intensities ($u>1$). A complete damping of optical modulations will take place when the $3d$ population after the first pulse is equal to zero. Thus, as far as its origin is concerned, the complete disappearance of optical modulations in this case is analogous to that considered previously in Sec. III A. The difference in physics is that now, in the $40f$ initial-state case, no population has been sent by the highly intense ($u\gg 1$) first pulse to the $3d$ state [Fig. 4(c)], while in the previous $3d$ initial-state case all population was removed by the first pulse from this $3d$ state [Fig. 2(d)].

We have also analyzed the redistribution of the initial $40f$ population by a laser pulse of duration different to that of $\tau=0.2$, considered up to now. In Fig. 6 we show an interesting result for a pulse of duration equal to half of a Kepler period, i.e., $\tau=0.5$. According to Fig. 6(a), the first pulse of this duration depletes the initially populated $40f$ Rydberg state more and more with increasing intensity, down to zero population at high intensities ($u>1$). The predicted result of this strong-field depletion of the initial $40f$ state by the first pulse should be a gradual disappearance of all Fourier-spectrum frequency components, corresponding to the eigenfrequency differences between the initial $40f$ Rydberg state and any other state. Figure 6(b) confirms this prediction; it gives the height, i.e., intensity, of the exemplifying $42f$-$40f$ frequency component in the $42f$ population variations against laser intensity. After the initial increase in the intensity of this frequency component we can observe its disappearance, starting from the threshold laser intensity determined by the condition $u\simeq 0.2$, and its almost complete disappearance at $u>1$. Such behavior of this exemplifying frequency component is a consequence of increasing depletion of the initial $40f$ state by the first pulse, as shown in Fig. 6(a). The above-mentioned effect

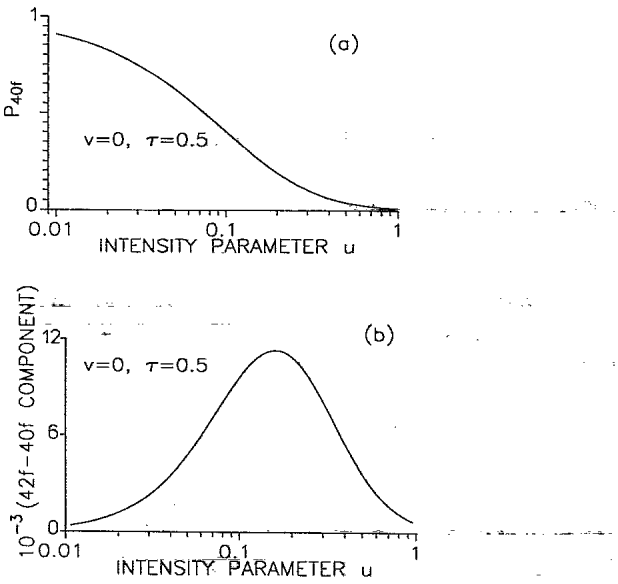

FIG. 6. (a) Population in the initial $40f$ Rydberg state after the first pulse versus the pulse intensity. (b) Intensity of the $42f$-$40f$ frequency component in the $42f$ population variations versus laser intensity. The pulse duration is equal to half the $40f$ Kepler period ($\tau=0.5$).

of the disappearance of low-frequency components in the spectrum is, as far as its origin is concerned, similar to that of the vanishing of the fast optical component discussed in Sec. III A. In both cases the reason for these phenomena is the complete depletion of the initial state (either $40f$ or $3d$). This high-intensity theoretical prediction is what we suggest should be tested in future experiments.

C. $40f$ initial-state case with ionization

Figure 7 shows the population variation in the $42f$ state, but under conditions completely different from

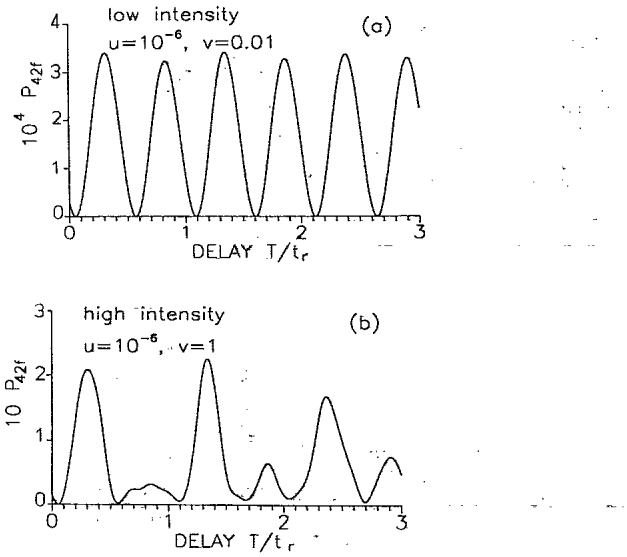

FIG. 7. Same as Fig. 4, but now with the $40f$-$3d$ channel closed ($u=10^{-6}$) and the redistribution channel via the continuum open ($v\neq 0$).

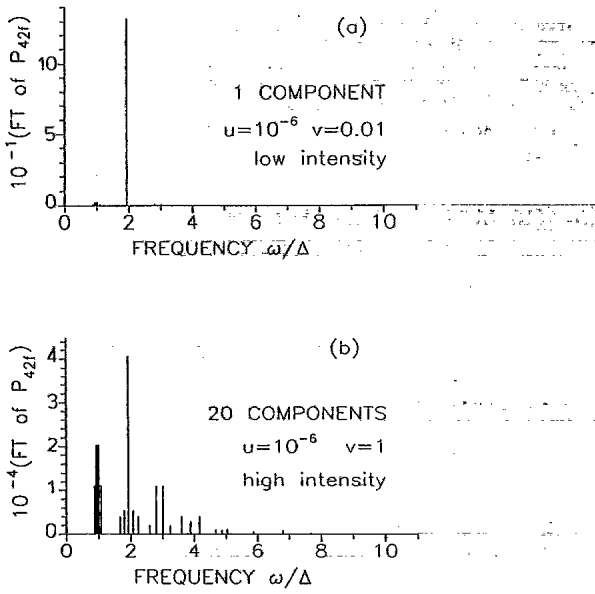

FIG. 8. Corresponding Fourier spectra of the time variations in Fig. 7.

those in Fig. 4. Figure 4 was obtained by neglect of the atomic continuum effect ($v=0$), while Fig. 7 shows the effect of the continuum in its pure form. The latter figure is made under practically negligible coupling of f Rydberg states to the lower $3d$ state ($u=10^{-6}$). In this case the only channel of redistribution of the initial $40f$ population are Raman transitions via the continuum between different Rydberg states. The growing effect of these Raman transitions with increasing laser intensity, from low ($v=0.01$) to high ($v=1$), is seen by comparing Fig. 7(a) with Fig. 7(b). The more complicated variation seen in Fig. 7(b) is the evidence of the redistribution of the initial $40f$ population over a large number of Rydberg states. The common feature of the two variations shown in Fig. 7 is a complete lack of rapid optical oscillations, as a result of practically no population sent to the lower $3d$ state below the Rydberg family by the first pulse. The appropriate Fourier spectrum, shown in Fig. 8, points to an increase in the number of frequency components with increasing intensity, from one component at the low intensity to 20 components at the high intensity. This increase is a clear demonstration of the Rydberg state redistribution due to the Raman processes via the continuum. The above theoretical result is consistent with the recent experiment of Noordam *et al.* [5], in which this kind of redistribution was observed in atomic barium. As it is known [5–16], such a redistribution via continuum is responsible for the so-called interference stabilization of the Rydberg atom against photoionization in intense laser fields.

As in Sec. III B, the effect of laser intensity observed in Figs. 7 and 8 can again be understood qualitatively as a result of interference of elementary transition paths involving different numbers of photons. Now, because of negligible coupling of f Rydberg states to the lower $3d$ state, it suffices to consider only two-photon direct paths and four-photon indirect paths. When compared with Sec. III B, the difference is that now the atomic continuum, rather than the discrete spectrum, is engaged in each Raman transition.

IV. SUMMARY

We have presented an analytically solvable model of population dynamics in a Rydberg atom, exposed to a sequence of two time separated, identical, short laser pulses. The solution we found covers both the perturbative case of weak depletion and the nonperturbative case of strong depletion of the initial state. From the variation of population in *only* one state, as a function of a delay between the pulses, and from the Fourier transformation of this variation, we have been able to draw conclusions about the effect of laser intensity on the redistribution of the initial population over a number of states. In qualitative agreement with the experiment of Jones *et al.* [3] for the potassium atom, our model points to a general increase in the number of states that take part in the redistribution with increasing intensity of a laser pulse. It has led us to the conclusion that a correct description of the redistribution in the high-intensity limit would require models with the number of states not overlimited. Our model points also to the importance of Raman transitions via the continuum in Rydberg-state redistribution, in agreement with the experiment of Noordam *et al.* [5] for the barium atom. Besides the qualitative explanations of the already existing experimental results, we have found such peculiar behavior of our theoretical Fourier spectrum of population variation in a given state that it deserves further experimental testing, i.e., our prediction of the disappearance of some frequency components (both low and optical) in the high-intensity spectrum due to depletion of the initial state by the first pulse. We hope that the results of this paper confirm that the Ramsey-like experimental technique of two identical, separated in time, short laser pulses in a good tool to study population dynamics and redistribution over a large number of states of a population that was initially in a single state.

ACKNOWLEDGMENT

This research was made possible thanks to the support from the Committee for Scientific Research under Grant No. 2 2338 92 03.

[1] W. Demtröder, *Laser Spectroscopy, Basic Concepts and Instrumentation* (Springer-Verlag, Berlin, 1988).

[2] N. F. Scherer, R. J. Carlson, A. Matro, M. Du, A. J. Ruggiero, V. Romero-Rochin, J. A. Cina, G. R. Fleming, and S. A. Rice, J. Chem. Phys. **95**, 1487 (1991); V. Engel and H. Metiu, *ibid.* **100**, 5448 (1994).

[3] R. R. Jones, C. S. Raman, D. W. Schumacher, and P. H. Bucksbaum, Phys. Rev. Lett. **71**, 2575 (1993).

[4] L. D. Noordam, D. I. Duncan, and T. F. Gallagher, Phys. Rev. A **45**, 4734 (1992).

[5] L. D. Noordam, H. Stapelfeldt, D. J. Duncan, and T. F. Gallagher, Phys. Rev. Lett. **68**, 1496 (1992).

[6] A. Wójcik and R. Parzyński, Phys. Rev. A **50**, 2475 (1994).
[7] M. V. Fedorov and A. M. Movsesian, J. Phys. B **21**, L155 (1988); J. Opt. Soc. Am. B **6**, 928 (1989); **6**, 1504 (1989); Zh. Eksp. Teor. Fiz. **95**, 47 (1989).
[8] J. Parker and C. R. Stroud, Jr., Phys. Rev. A **40**, 5651 (1989); **41**, 1602 (1990).
[9] M. V. Fedorov, M. Yu. Ivanov, and P. B. Lerner, J. Phys. B **23**, 2505 (1990).
[10] M. V. Fedorov, M. Yu. Ivanov, and A. M. Movsesian, J. Phys. B **23**, 2245S (1990).
[11] P. R. Jones and P. H. Bucksbaum, Phys. Rev. Lett. **67**, 3215 (1991).
[12] H. Stapelfeldt, D. G. Papaioannou, L. D. Noordam, and T. F. Gallagher, Phys. Rev. Lett. **67**, 3223 (1991).
[13] L. Roso-Franco, G. Orriols, and J. H. Eberly, Laser Phys. **2**, 741 (1992).
[14] K. Burnett, V. C. Reed, and P. L. Knight, J. Phys. B **26**, 561 (1993).
[15] A. Scrinzi, N. Elander, and B. Piraux, Phys. Rev. A **48**, R2527 (1993).
[16] M. P. de Boer, J. H. Hoogenraad, R. B. Vrijen, L. D. Noordam, and H. G. Muller, Phys. Rev. Lett. **71**, 3263 (1993).
[17] C. E. Caroll and F. T. Hioe, Phys. Rev. A **47**, 571 (1993).
[18] C. E. Theodosiou, Phys. Rev. A **30**, 2881 (1984).